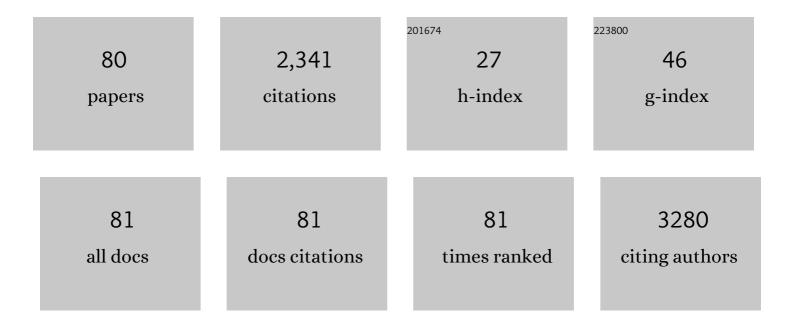
List of Publications by Year in descending order

Source: https://exaly.com/author-pdf/3703562/publications.pdf Version: 2024-02-01



ΥΠ-ΠΗΝ ΟΙΝ

#	Article	IF	CITATIONS
1	PVK-Modified Single-Walled Carbon Nanotubes with Effective Photoinduced Electron Transfer. Macromolecules, 2003, 36, 6286-6288.	4.8	176
2	Carbon Nanotube Delivery of the GFP Gene into Mammalian Cells. ChemBioChem, 2006, 7, 239-242.	2.6	156
3	Reduction of solubilized multi-walled carbon nanotubes. Carbon, 2003, 41, 331-335.	10.3	125
4	Large-Scale Preparation of Solubilized Carbon Nanotubes. Chemistry of Materials, 2003, 15, 3256-3260.	6.7	109
5	Electrical Properties of Soluble Carbon Nanotube/Polymer Composite Films. Chemistry of Materials, 2005, 17, 130-135.	6.7	106
6	Concise Route to Functionalized Carbon Nanotubes. Journal of Physical Chemistry B, 2003, 107, 12899-12901.	2.6	93
7	Effect of Surfactant Structure on the Stability of Carbon Nanotubes in Aqueous Solution. Journal of Physical Chemistry B, 2008, 112, 7227-7233.	2.6	77
8	Noncovalent assembly of carbon nanotube-inorganic hybrids. Journal of Materials Chemistry, 2011, 21, 7527.	6.7	74
9	Reduced Defects of MAPbI ₃ Thin Films Treated by FAI for Highâ€Performance Planar Perovskite Solar Cells. Advanced Functional Materials, 2019, 29, 1805810.	14.9	73
10	Efficient method to functionalize carbon nanotubes with thiol groups and fabricate gold nanocomposites. Chemical Physics Letters, 2005, 401, 352-356.	2.6	72
11	In situ synthesis of CdS nanoparticles on multi-walled carbon nanotubes. Carbon, 2004, 42, 455-458.	10.3	66
12	Fabrication and Characterization of Soluble Multi-Walled Carbon Nanotubes Reinforced P(MMA-co-EMA) Composites. Macromolecular Materials and Engineering, 2004, 289, 828-832.	3.6	63
13	Adverse Effects of Excess Residual PbI ₂ on Photovoltaic Performance, Charge Separation, and Trap‣tate Properties in Mesoporous Structured Perovskite Solar Cells. Chemistry - A European Journal, 2017, 23, 3986-3992.	3.3	63
14	Carbon nanotube composite microspheres as a highly efficient solid-phase microextraction coating for sensitive determination of phthalate acid esters in water samples. Journal of Chromatography A, 2016, 1468, 17-22.	3.7	62
15	C60 modified single-walled carbon nanotubes. Chemical Physics Letters, 2003, 377, 32-36.	2.6	59
16	Facile fabrication of binder-free reduced graphene oxide/MnO2/Ni foam hybrid electrode for high-performance supercapacitors. Journal of Alloys and Compounds, 2020, 812, 152124.	5.5	55
17	Facile preparation of graphene/polyaniline composite hydrogel film by electrodeposition for binder-free all-solid-state supercapacitor. Journal of Alloys and Compounds, 2021, 875, 159931.	5.5	44
18	Multiwalled Carbon Nanotube Microspheres from Layer-by-Layer Assembly and Calcination. Journal of Physical Chemistry C, 2008, 112, 11617-11622.	3.1	37

#	Article	lF	CITATIONS
19	Trap-limited charge recombination in intrinsic perovskite film and meso-superstructured perovskite solar cells and the passivation effect of the hole-transport material on trap states. Physical Chemistry Chemical Physics, 2015, 17, 29501-29506.	2.8	36
20	Porous gold nanoparticle/graphene oxide composite as efficient catalysts for reduction of 4-nitrophenol. RSC Advances, 2016, 6, 35945-35951.	3.6	35
21	Self-Assembly of Gold Nanoparticles on Fullerene Nanospheres. Langmuir, 2004, 20, 1466-1472.	3.5	34
22	Hollow Carbon Nanotube Microspheres and Hemimicrospheres. Journal of Physical Chemistry C, 2009, 113, 1666-1671.	3.1	33
23	Evaporation-induced hydrated graphene/polyaniline/carbon cloth integration towards high mass loading supercapacitor electrodes. Chemical Engineering Journal, 2022, 445, 136727.	12.7	33
24	Dumb-belled PCBM derivative with better photovoltaic performance. Journal of Materials Chemistry, 2012, 22, 1758-1761.	6.7	32
25	Alkylation and arylation of single-walled carbon nanotubes by mechanochemical method. Chemical Physics Letters, 2007, 444, 258-262.	2.6	31
26	<i>In Situ</i> Synthesis of Trifluoroacetic Acid-Doped Polyaniline/Reduced Graphene Oxide Composites for High-Performance All-Solid-State Supercapacitors. ACS Applied Energy Materials, 2020, 3, 8774-8785.	5.1	29
27	Optical limiting performances of multi-walled carbon nanotubols and [C60]fullerols. Chemical Physics Letters, 2008, 457, 159-162.	2.6	28
28	Mechanism of biphasic charge recombination and accumulation in TiO ₂ mesoporous structured perovskite solar cells. Physical Chemistry Chemical Physics, 2016, 18, 12128-12134.	2.8	28
29	Metal-organic framework-derived Mn3O4 nanostructure on reduced graphene oxide as high-performance supercapacitor electrodes. Journal of Alloys and Compounds, 2022, 897, 162640.	5.5	25
30	Modification of NiOx hole transport layer for acceleration of charge extraction in inverted perovskite solar cells. RSC Advances, 2020, 10, 12289-12296.	3.6	22
31	Charge carrier recombination dynamics in a bi-cationic perovskite solar cell. Physical Chemistry Chemical Physics, 2019, 21, 5409-5415.	2.8	20
32	The pH-controlled morphology transition of polyaniline from nanofibers to nanospheres. Nanotechnology, 2013, 24, 175602.	2.6	19
33	Effects of interfacial energy level alignment on carrier dynamics and photovoltaic performance of inverted perovskite solar cells. Journal of Power Sources, 2020, 452, 227845.	7.8	19
34	Influence of the MACI additive on grain boundaries, trap-state properties, and charge dynamics in perovskite solar cells. Physical Chemistry Chemical Physics, 2021, 23, 6162-6170.	2.8	18
35	Covalently attached multilayer self-assemblies of single-walled carbon nanotubols and diazoresins. Nanotechnology, 2007, 18, 365704.	2.6	17
36	The influence of morphology on charge transport/recombination dynamics in planar perovskite solar cells. Chemical Physics Letters, 2016, 662, 257-262.	2.6	17

#	Article	IF	CITATIONS
37	Convenient fabrication of graphene/gold nanoparticle aerogel as direct electrode for H2O2 sensing. Materials Letters, 2017, 207, 49-52.	2.6	17
38	Rational design of active layer configuration with parallel graphene/polyaniline composite films for high-performance supercapacitor electrode. Electrochimica Acta, 2021, 398, 139330.	5.2	17
39	Preparation of carbon nanotube/chitosan/gold nanoparticle composite microspheres. Materials Letters, 2011, 65, 1510-1513.	2.6	16
40	The influence of the electron transport layer on charge dynamics and trap-state properties in planar perovskite solar cells. RSC Advances, 2020, 10, 12347-12353.	3.6	16
41	Gold nanoparticles/carbon nanotubes composite microspheres for catalytic reduction of 4-nitrophenol. Chinese Chemical Letters, 2016, 27, 843-846.	9.0	15
42	Efficient promotion of charge separation and suppression of charge recombination by blending PCBM and its dimer as electron transport layer in inverted perovskite solar cells. RSC Advances, 2016, 6, 112512-112519.	3.6	15
43	The Influence of Structural Configuration on Charge Accumulation, Transport, Recombination, and Hysteresis in Perovskite Solar Cells. Energy Technology, 2017, 5, 442-451.	3.8	15
44	Solvent-free mechanochemical synthesis of diacylfuroxans. Tetrahedron Letters, 2019, 60, 1687-1690.	1.4	14
45	Graphene/Gold nanoparticle composite-based paper sensor for electrochemical detection of hydrogen peroxide. Fullerenes Nanotubes and Carbon Nanostructures, 2019, 27, 23-27.	2.1	13
46	Solvent effects of optical limiting properties of carbon nanotubes. Synthetic Metals, 2003, 135-136, 853-854.	3.9	12
47	Ultrafast third-order nonlinear optical response of two soluble multi-wall carbon nanotubes. Journal Physics D: Applied Physics, 2004, 37, 1079-1082.	2.8	12
48	A convenient approach to producing a sensitive MWCNT-based paper sensor. RSC Advances, 2016, 6, 112241-112245.	3.6	12
49	Photovoltaic properties of dimeric methanofullerenes containing hydroxyl groups. Chemical Physics Letters, 2012, 535, 100-105.	2.6	11
50	Strengthened graphene oxide/diazoresin multilayer composites from layer-by-layer assembly and cross-linking. Chinese Chemical Letters, 2015, 26, 1155-1157.	9.0	11
51	Multipleâ€Trapping Model for the Charge Recombination Dynamics in Mesoporousâ€Structured Perovskite Solar Cells. ChemSusChem, 2017, 10, 4872-4878.	6.8	11
52	Characterization of the influences of morphology on the intrinsic properties of perovskite films by temperature-dependent and time-resolved spectroscopies. Physical Chemistry Chemical Physics, 2018, 20, 6575-6581.	2.8	11
53	Fabrication of multi-walled carbon-nanotube-grafted polyvinyl-chloride composites with high solar-thermal-conversion performance. Composites Science and Technology, 2019, 170, 77-84.	7.8	11
54	Cross-linked multilayer composite films and microcapsules embedded carbon nanotubes. Materials Letters, 2013, 105, 132-135.	2.6	10

#	Article	IF	CITATIONS
55	Effect of energetic distribution of trap states on fill factor in perovskite solar cells. Journal of Power Sources, 2020, 479, 229077.	7.8	10
56	Charge Photogeneration Dynamics of Poly(3-hexylthiophene) Blend with Covalently-Linked Fullerene Derivative in Low Fraction. Journal of Physical Chemistry C, 2014, 118, 21377-21384.	3.1	9
57	Graphene/gold nanoparticle aerogel electrode for electrochemical sensing of hydrogen peroxide. Materials Letters, 2018, 229, 368-371.	2.6	9
58	Bifunctional Chlorosilane Modification for Defect Passivation and Stability Enhancement of High-Efficiency Perovskite Solar Cells. Journal of Physical Chemistry C, 2020, 124, 22903-22913.	3.1	8
59	Graphene Hydrogels Implanted onto Carbon Cloth for Polypyrrole Electrodeposition toward High-Performance Supercapacitor Electrodes. ACS Sustainable Chemistry and Engineering, 2022, 10, 8495-8505.	6.7	8
60	The Influence of Morphology and PbI ₂ on the Intrinsic Trap State Distribution in Perovskite Films Determined by Using Temperatureâ€Đependent Fluorescence Spectroscopy. ChemPhysChem, 2017, 18, 310-317.	2.1	7
61	Simultaneous Transport Promotion and Recombination Suppression in Perovskite Solar Cells by Defect Passivation with Li-Doped Graphitic Carbon Nitride. Journal of Physical Chemistry C, 2021, 125, 5525-5533.	3.1	7
62	Polarization-Induced Trap States in Perovskite Solar Cells Revealed by Circuit-Switched Transient Photoelectric Technique. Journal of Physical Chemistry C, 2022, 126, 3696-3704.	3.1	7
63	Characterization and Distribution of Poly(3â€hexylthiophene) Phases in an Annealed Blend Film. ChemPhysChem, 2014, 15, 935-941.	2.1	6
64	Preparation of graphene/Au aerogel film through the hydrothermal process and application for H ₂ O ₂ detection. RSC Advances, 2019, 9, 13042-13047.	3.6	6
65	The influence of hierarchical TiO2 microspheres on the trap state distribution and charge transport/recombination dynamics in quantum dot sensitized solar cells. RSC Advances, 2015, 5, 32110-32117.	3.6	5
66	The influence of fullerene on hysteresis mechanism in planar perovskite solar cells. Chemical Physics Letters, 2020, 750, 137443.	2.6	5
67	The fabrication of flower-like graphene/octadecylamine composites. Chinese Chemical Letters, 2015, 26, 1144-1146.	9.0	4
68	Power output and carrier dynamics studies of perovskite solar cells under working conditions. Physical Chemistry Chemical Physics, 2017, 19, 19922-19927.	2.8	4
69	Preparation and Properties of Polyvinyl Chloride/Carbon Nanotubes Composite. Journal Wuhan University of Technology, Materials Science Edition, 2019, 34, 516-520.	1.0	4
70	An Electrogenerated Chemical-Oxidation-Driving Nonvolatile Plastic Memory Device with the Conjugated Polymer/Carbon Nanotube Blend. Electrochemical and Solid-State Letters, 2007, 10, P19.	2.2	3
71	Facile fabrication of 1,3-diazaazulene derivative nanowires. Materials Letters, 2017, 205, 182-185.	2.6	3
72	Protonation behaviour of 2-phenyl-1,3-diazaazulene derivatives. Tetrahedron, 2018, 74, 731-739.	1.9	3

#	Article	IF	CITATIONS
73	Facile synthesis of diarylsulfones from arenes and 3CdSO4·xH2O via mechanochemistry. Tetrahedron Letters, 2020, 61, 151567.	1.4	3
74	Mechanochemical sulfonation of aromatic compounds using NaHSO4·H2O/P2O5. Journal of Chemical Research, 0, , 174751982110325.	1.3	2
75	Diffusion Dynamics of Mobile Ions Hidden in Transient Optoelectronic Measurement in Planar Perovskite Solar Cells. ACS Applied Energy Materials, 2020, 3, 8330-8337.	5.1	1
76	Fabrication of PVC/MWNTs-g-C16 composites with high solar-thermal conversion performance for anti-icing and deicing. ScienceAsia, 2020, 46, 169.	0.5	1
77	Silicon Dioxide Nanoparticles Increase the Incidence Depth of Short-Wavelength Light in Active Layer for High-Performance Perovskite Solar Cells. Journal of Physical Chemistry C, 2022, 126, 7400-7409.	3.1	1
78	Synthesis, crystal structure and photophysical properties of 1,4-bis(1,3-diazaazulen-2-yl)benzene: a new Ĩ€ building block. Acta Crystallographica Section C, Structural Chemistry, 2018, 74, 171-176.	0.5	0
79	Ferric chloride–catalyzed deoxygenative chlorination of carbonyl compounds: A comparison of chlorodimethylsilane and dichloromethylsilane system. Journal of Chemical Research, 2020, 44, 667-675.	1.3	0
80	Interpretation of the Biphasic Charge Carrier Recombination Process Observed in Mesoporous-Structured Perovskite Solar Cells. , 0, , .		0